serac: an R package for ShortlivEd RAdionuclide chronology of recent sediment cores

Rosalie Bruel, Pierre Sabatier

serac: a R package for ShortlivEd RAdionuclide Chronology of recent sediment cores

Bruel Rosalie[1,2,*] and Sabatier Pierre[3]

[1]CARRTEL, Université Savoie-Mont Blanc, INRA, 74200 Thonon-les-Bains, France

[2]Rubenstein Ecosystem Science Laboratory, University of Vermont, 05401 Burlington VT, USA

[3]EDYTEM, Université Savoie-Mont Blanc, CNRS, 73370, Le Bourget du Lac, France

[*]corresponding author: rosaliebruel@gmail.com

serac: a R package for ShortlivEd RAdionuclide Chronology of recent sediment cores

Abstract

Short-lived radionuclides are measured in surface sediment to provide a geochronology for the past century. Age-depth models are produced from $^{210}Pb_{ex}$ activity-derived sedimentation rates and confirmed by ^{137}Cs and ^{241}Am activities that are result of fallout from nuclear weapon tests and the Chernobyl accident. Different methods of age depth modelling using such data require expertise in lake sedimentation processes.

Here, we present a package, *serac*, that allows the user to compute an age-depth model, output a graph and an age model as a text file, and provide metadata using the free open-source statistical software R. *serac* ensures the reproducibility of age-depth or age-mass depth models and allows testing of several ^{210}Pbex models (CFCS, CIC, CRS, CRS piecewise) and sedimentation hypotheses (changes in the sedimentation rates, instantaneous deposits, varved sedimentation, etc.). Using several case studies, including lakes and lagoon in different environments, we demonstrate the use of the programme in diverse situations that may be encountered.

The rising number of sediment cores in recent palaeo-studies and the need to correlate them require reproducible methods. *serac* is a user-friendly code that enables age model computation for the past century and encourages the standardisation of outputs.

Keywords: Shortlived radionuclide; R package; ^{210}Pb model; ^{137}Cs; age model; metadata

1. Introduction

Dating sediments is the first and critical step of any palaeo-study. Specifically, accurately dating the past century is crucial in palaeoclimate and palaeoecological studies because of the many socio-ecological changes that took place during that period. Furthermore, there is a great amount of instrumental and historical data (e.g., floods, changes in land use) available for the past century, and a precise age-model is needed to correlate these observational data to sediment proxies. When annual varves are absent, short-lived radionuclides, based on the measurements of the activity of ^{137}Cs, ^{241}Am, ^{210}Pb, and ^{226}Ra, provide the most accurate and widely used age-depth model technique for the past century.

The isotopes ^{137}Cs ($t_{1/2}$= 30.15 years) and ^{241}Am ($t_{1/2}$= 432 years) are by-products from nuclear weapons tests conducted from 1955 and for a decade, by the United-States, the former URSS, and the United Kingdom. The isotope ^{137}Cs peaked in 1963, and was accompanied by a smaller peak in ^{241}Am, itself resulting from the decay of ^{241}Pu ($t_{1/2}$= 14 years), one of the elements in fallout from atmospheric nuclear weapons tests. The Chernobyl accident in 1986 further dispersed ^{137}Cs into the atmosphere of the northern hemisphere (Appleby et al., 1991). Independent of human activities, ^{210}Pb excess activity is used to estimate environmental sedimentation dynamics. The basic methodology of ^{210}Pb dating was first established in a seminal paper by Goldberg (1963). ^{210}Pb is an isotope of lead that forms during the decay sequence of ^{238}U. ^{210}Pb results from the disintegration of ^{226}Ra in rock, sediments and water, and from the disintegration of ^{222}Rn in the atmosphere (Fig. 1). While ^{226}Ra and ^{210}Pb triggered by erosion in the watershed are in secular equilibrium (^{210}Pb supported), the ^{210}Pb produced in the atmosphere by ^{222}Rn decay are removed from the atmosphere by dry and wet fallout and are integrated in soils, lakes and sediments (Fig. 1, excess ^{210}Pb, referred to hereafter as $^{210}Pb_{ex}$). As a consequence, it is possible to estimate the atmospheric $^{210}Pb_{ex}$ by subtracting the total ^{210}Pb ($^{210}Pb_{mes}$) by ^{226}Ra. The $^{210}Pb_{ex}$ activity follows an exponential decay (characterised by its half-life $t_{1/2}$= 22.3 years) from which it is possible to calculate age and sedimentation rates for the past 100 to 150 years (~5 x $t_{1/2}$, eq. 1).

$$^{210}Pb_{ex}^{z} = {}^{210}Pb_{ex}^{0} \times e^{-\lambda t} \quad \text{with} \quad {}^{210}Pb_{ex} = {}^{210}Pb_{mes} - {}^{226}Ra_{mes} \quad (1)$$

where t is the age at depth z, $^{210}Pb^{0}_{ex}$ is the activity at the surface of the sediment express in $Bq.kg^{-1}$ or $mBq.g^{-1}$, $^{210}Pb^{z}_{ex}$ is the activity at depth z and λ the ^{210}Pb disintegration constant (ln(2)/22.3; expressed in y^{-1}).

The isotopes ^{137}Cs, ^{241}Am, ^{210}Pb, and ^{226}Ra are most commonly measured together using a non-destructive gamma-spectrometric analysis, allowing a direct determination of ^{210}Pb supported through the ^{226}Ra activity. ^{210}Pb can also be quantified by alpha-spectrometry determination of its daughter ^{210}Po ($t_{1/2}$= 138 d). Isotopes are used in chronologies for lake sediment (Rapuc et al., 2018; Sabatier et al., 2014), lagoons (Sabatier et al., 2010a), but also corals (Andrews et al., 2009; Druffel et al., 1990; Moore and Krishnaswami, 1972; Sabatier et al., 2012) and speleothems (Baskaran and Iliffe, 1993; Condomines and Rihs, 2006) through excess or ingrowth methods.

Several models to infer ages from $^{210}Pb_{ex}$ decay have been proposed over time (Appleby, 2008, 2001; Appleby and Oldfield, 1992; Arias-Ortiz et al., 2018; Sanchez-Cabeza and Ruiz-Fernández, 2012), none of which can be considered as an universal method as the best model must be chosen with consideration to potential variability in watershed erosional input, and ideally, by validating the model with independent markers (Baskaran et al., 2014; Binford, 1990; Cooke et al., 2010; Kirchner, 2011). While there is no doubt, the complexity and heterogeneity of sedimentation processes calls for permanent progression of models (Abril Hernández, 2016) and uncertainties estimations (Aquino-López et al., 2018), the method for the most classic model is so well established that many geochronologist teams working on recent records confidently use it. The downside of its success is that there is often a lack of information on sedimentation hypotheses in published age-depth models (Blaauw, 2010), as if mentioning the method certified the age model accuracy. While we are not questioning the validity of every published model, any field benefits from transparency to allow for reproducibility of its results (Wilkinson et al., 2016).

As establishing an age-depth model is the first step of any investigation on sediment sequences, ensuring the hypotheses made at this stage are transparent is critical. Blaauw (2010) provided the *clam* R code to the palaeo-community to provide an easy, automated, transparent, documented, and adaptable environment for producing age-models from ^{14}C sequences. Routines in Excel and Matlab exist for some of the ^{210}Pb models (Abril Hernández, 2016), and a promising Bayesian ^{210}Pb model based on constant rate of supply (CRS) is available as a R package (*plum*) (Aquino-López et al., 2018). Herein, we propose a systematic approach to producing chronologies for sediment cores using short-lived radionuclides ($^{210}Pb_{ex}$, ^{137}Cs and ^{241}Am) and different types of $^{210}Pb_{ex}$ models (constant initial concentration (CIC), constant rate of supply (CRS), constant flux constant sedimentation rate (CFCS), and piecewise versions of CRS and CFCS), based on the free and open-source software R. We first describe the different hypotheses for $^{210}Pb_{ex}$ decay and the resulting models; we then introduce the elements of the R function we developed, before applying the *serac* code to six complex case studies. Eventually, we wish our code to supplement *clam* for chronologies for the past century.

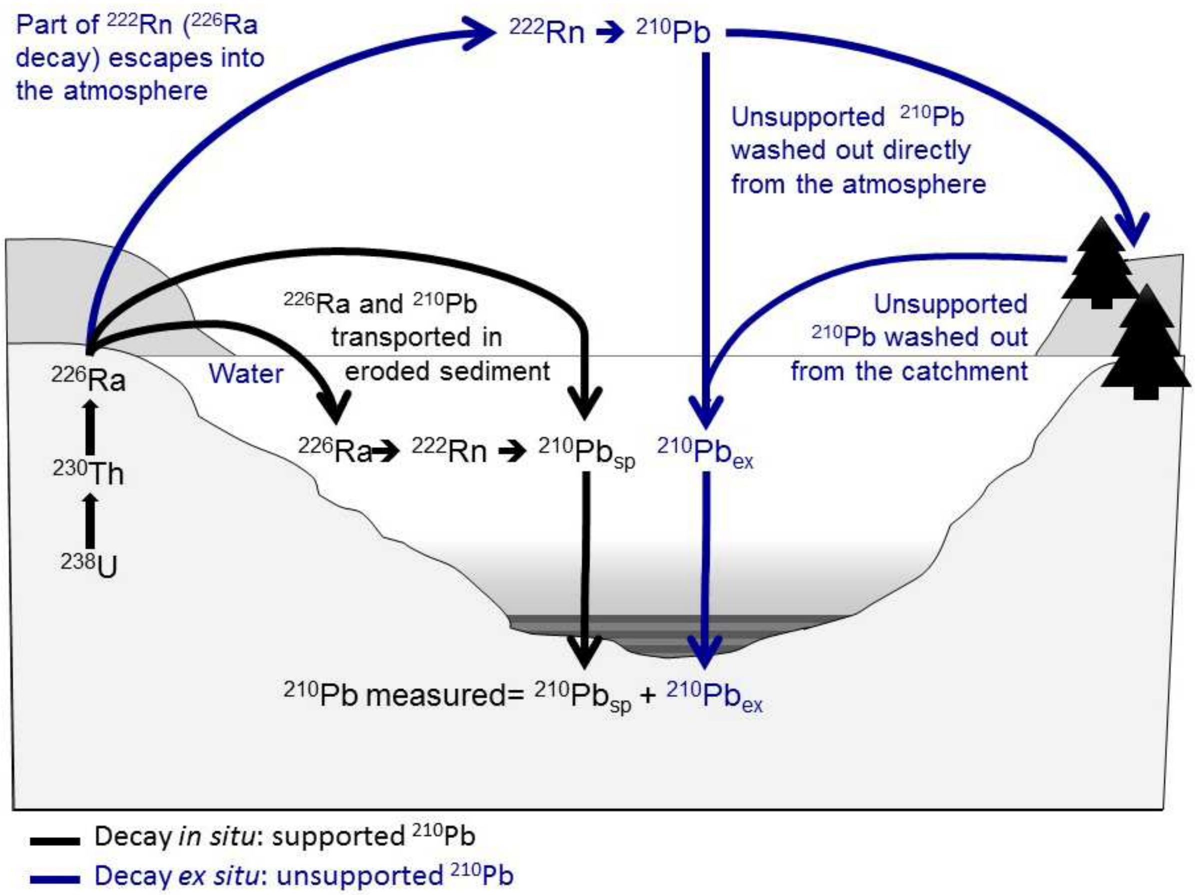

Figure 1. ^{210}Pb sources in lake or marine environments

2. ^{210}Pb-based radiometric dating models

serac allows computation of the 3 most common models (Appleby, P.G. and Oldfield, F., 1992), CIC, CFCS, CRS, as well as the piecewise version of CRS (age and depth forced) and CFCS (when instantaneous deposits are present). The models share the initial assumptions: i) radionuclides are particle-bound tracers which are ideally deposited onto the sediment-water interface, ii) non-post depositional redistribution takes place except in the surface mixed layer, and iii) the sedimentary sequence is continuous. Each model has then other varying assumptions regarding ^{210}Pbex fluxes and sedimentation rates. The models and other assumptions are detailed below (Table 1).

Table 1. Summary of the assumptions for $^{210}Pb_{ex}$ models included in serac. CIC, CFCS and CRS respectively stand for constant initial concentration, constant flux constant sedimentation rate and constant rate of supply.

Assumption	CIC	CFCS	CRS	CRS piecewise
Radionuclides deposition	Homogeneously deposition onto the sediment-water interface and particle bound.			
Non-post depositional redistribution takes place (except in the surface mixed layer)	x (Does not handle surface mixed layer)	x	x	x
Sedimentary sequence	Continuous	Continuous	Continuous	Continuous
$^{210}Pb_{ex}$ fluxes	Increases when sedimentation rate decreases, and *vice versa*.	Constant	Constant	Could change
Sedimentation rates	Decreases when $^{210}Pb_{ex}$ fluxes increases, and *vice versa*.	Constant	Varies	Varies
Compaction	Use mass-depth instead of depth	Use mass-depth instead of depth	Use mass-depth instead of depth	Use mass-depth instead of depth

2.1. Constant Initial Concentration

The constant initial concentration (CIC) model is based on the hypothesis that any changes in $^{210}Pb_{ex}$ flux or the sedimentation rate are synchronous and reversed so that the initial activity within the sediment remain constant (Pennington et al., 1976). The model relies on the following equation:

$$t_z = \frac{1}{\lambda} \times ln\left[\frac{^{210}Pb_{ex}^{0}}{^{210}Pb_{ex}^{z}}\right] \qquad (2)$$

where t_z is the age at depth z, $^{210}Pb^{0}_{ex}$ is the activity at the surface of the sediment, and $^{210}Pb^{z}_{ex}$ is the activity at depth z. This model cannot be used if bioturbation has affected the sediment column or if an instantaneous event perturbed the $^{210}Pb_{ex}$ decrease profile (low $^{210}Pb_{ex}$ values). Uncertainties in the CIC model derived ages are computed from equations from Sanchez-Cabeza and Ruiz-Fernández, (2012).

2.2. Constant Flux Constant Sedimentation

The constant flux constant sedimentation rate (CFCS) model method is based on the hypothesis that there is neither mixing nor Pb diffusion in the sediment (Goldberg, 1963; Krishnaswamy et al., 1971). In a semilogarithmic diagram $^{210}Pb_{ex}$ activities relative to the depth have a linear relationship, as follows:

$$\text{From (1) :} \qquad \ln(^{210}Pb^{z}_{ex}) = \ln(^{210}Pb^{0}_{ex}) - \lambda\frac{z}{SAR} \quad with \quad t = \frac{z}{SAR} \qquad (3)$$

$^{210}Pb_{ex}^{0}$ is the $^{210}Pb_{ex}$ activity at the sediment surface (t=0), z is the depth and *SAR* is the sediment accumulation rate expressed in (mm.yr^{-1}). Any instantaneous event has to be removed before computation (low $^{210}Pb_{ex}$ values). In the *serac* package, this model supports up to two changes in sedimentation rate.

To take into account compaction process, age model can be computed as a function of mass depth (m_z, g.cm^{-2}) instead of depth (z, mm) with:

$$m_z = \sum_{j=0}^{j=i} DBD_j \times \Delta z_j \quad with \quad DBD_j = \frac{\Delta m_j}{S\Delta z_j} \quad (4)$$

Dry bulk densities (DBD, g.cm^{-3}) for each section is required to compute MAR; Δz is the section width and S is the core cross section (cm^2). Then, sedimentation rates are then expressed as mass accumulation rates (MAR) in (g.cm^{-2}.y^{-1}). The CFCS model applied versus mass depth (by cluster or not) presents a very interesting alternative to CRS model (Abril, 2019; Tylmann et al., 2016). DBD relative uncertainties are fixed at 7% as suggested by Appelby (2001).

2.3.Constant Rate of Supply

The constant rate of supply (CRS) model is based on the hypotheses that $^{210}Pb_{ex}$ (P) flux is constant, but the SAR varies with time (Appleby and Oldfield, 1978). As a result, the ^{210}Pbex activity decreases when sediment fluxes increase. This model defined the cumulative activity A(t) (mBq.cm^{-2}) during time t, corresponding to a depth z, as follows:

$$A(t) = \int_0^t P(t).\partial t \quad (5)$$

The $^{210}Pb_{ex}$ inventory can then be calculated (6) by taking in account the decay of $^{210}Pb_{ex}$ over time, as follows:

$$I = P_0 \int_0^{\infty} e^{-\lambda t} \partial t = \frac{P_0}{\lambda} = \sum_{z=0}^{\infty} (^{210}Pb)_{ex}^{z} \, m_z \quad (6)$$

where $\sum_{z=0}^{\infty} (^{210}Pb)_{ex}^{z} \, m_z$ represents the ^{210}Pbex activity integrated over the total sediment column until ^{210}Pbex reaches equilibrium, and m_z is the dry mass depth thickness of the measured section at z depth, express in g.cm^{-2}. If the section dry masses (m_Z) are not known, but we know those of the section DBD, the mass depths m_z can be calculated as:

$$m_j = DBD \times \Delta z_j \quad (7)$$

The use of this model assumes that all depths are measured (or interpolated) and that secular equilibrium is reached (i.e., no more $^{210}Pb_{ex}$ activities are observed in the deeper sample). The age (t_Z) at the depth Z is obtained by the equation (8), as follows:

$$t_Z = \frac{1}{\lambda} \times ln\left[\frac{\sum_{z=0}^{\infty}(^{210}Pb)_{ex}^{z} m_z}{\sum_{z=Z}^{\infty}(^{210}Pb)_{ex}^{z} m_z}\right] \quad (8)$$

where $\sum_{z=Z}^{\infty}(^{210}Pb)_{ex}^{z}\, m_z$ represents the $^{210}Pb_{ex}$ activity integrated below depth Z.

When the CRS model is applied, a "too-old" age error described by Binford (1990) is always present for the deeper core sections. The "too-old" age error arises from underestimation of $^{210}Pb_{ex}$ and may result from analytical limitations, sampling strategy or both. This underestimation is that their $^{210}Pb_{ex}$ ages are older than their true ages, hence the name "too-old" age error. Thus, $^{210}Pb_{ex}$ dating based on the CRS model must be conducted with caution (Blais et al., 1995) or corrected for (Tylmann et al., 2016) by reference age (Appleby, 2001) to avoid "too-old" age error for deeper core sections (Binford, 1990). Uncertainties in the CRS model derived ages are computed from equations from Sanchez-Cabeza and Ruiz-Fernández (2012).

Discrepancies between the derived CRS model and independent dates (from ^{137}Cs peak for example) can indicate variations in $^{210}Pbex$ flux. Appleby (2001) proposes a piecewise CRS model for cases where the fluxes pre and post-dating of a known reference date (1986 and 1963 AD artificial fallouts) are different. This model was then successively applied (Abril, 2019; Putyrskaya et al., 2020; Tylmann et al., 2016). If z1 and z2 are the depths of the two ^{137}Cs peaks dated at t1 (1986) and t2 (1963) or between the sampling year and a ^{137}Cs peak in the core and the mean $^{210}Pbex$ flux (P) during the period is:

$$P = \frac{\lambda \sum_{z=z1}^{z2}(^{210}Pb)_{ex}^{z} m_z}{e^{-\lambda t1} - e^{-\lambda t2}} \quad (9)$$

Where $\sum_{z=z1}^{z2}(^{210}Pb)_{ex}^{z}\, m_z$ is the $^{210}Pb_{ex}$ inventory between z1 and z2. Assuming the flux to be uniform within the identified section, dates and sedimentation rates for intermediate depths can be calculated by applying the principles of the CRS model with the flux calculated form (8). From the CRS model equations, having calculated P for this interval, the age t of the depth z between z1 and z2 is determined by the following equation:

$$t_Z = -\frac{1}{\lambda} \ln\left(e^{-\lambda t1} + \frac{\lambda}{P}\sum_{z}^{z2}(^{210}Pb)_{ex}^{z}\, m_z\right) \quad (10)$$

Where $\sum_{z}^{z2}(^{210}Pb)_{ex}^{z}\, m_z$ is the $^{210}Pb_{ex}$ inventory between z (the dated depth) and z2. The piecewise CRS age of a sediment horizon in the interval (t2, ∞) is given by Abril (2019) by the following equation:

$$t_Z = t_2 + \frac{1}{\lambda} \ln\left(\frac{\sum_{z2}^{\infty}(^{210}Pb)_{ex}^{z} m_z}{\sum_{z}^{\infty}(^{210}Pb)_{ex}^{z} m_z}\right) (11)$$

Such model could be applied for more than 2 known reference dates such historical events (pollution, flood, artificial fallouts, etc). Uncertainties for this last model are derived from analytical propagated error.

The classic $^{210}Pb_{ex}$ models (CIC, CFCS, CRS) included in *serac* are not adapted for situations with a continuous trend of change (increase/decrease) in fluxes and/or sedimentation rates which can be encountered in perturbed aquatic sedimentary systems. Many other models exist and have recently been summarized in Arias-Ortiz et al., (2018). More complex models allow for example for independent variability in $^{210}Pb_{ex}$ fluxes and sedimentation rates such as SIT (Sediment Isotope Tomography) (Carroll and Lerche, 2003), but also for statistical correlation between ^{210}Pbex fluxes and sedimentation rates (Abril Hernández, 2016). Other models can apply when deposition is non-ideal or when there is diffusion or mixing (Abril and Gharbi, 2012; Robbins et al., 1977). The piecewise version of classic models (CFCS, CRS) are well suited in cases with stepped changes in the sedimentary conditions (Abril, 2020, 2019); and serac allows these piecewise applications, as demonstrated in some of the case studies thereafter.

3. R code

We developed a package on the open-source software R (R Core Team, 2020). The package can be downloaded from the GitHub repository https://github.com/rosalieb/serac, or with the package *devtools* (Wickham et al., 2018) and the code:

```
library(devtools)
devtools::install_github("rosalieb/serac", build_vignettes = TRUE)
library(serac)
```

The package includes several function allowing to prepare the input file, generate age model, edit metadata, and create a map locating systems of interest (Table 2). This section focuses on the main function allowing to generate age depth model, *serac().*

In any given working directory (e.g., *~/serac*, but the working directory can bear any name the user chooses), a folder called "Cores" must be created. The input files must then be placed in a sub-folder of the "Cores" folder, e.g., *~/serac/Cores/MyCore/MyCore.txt*. Table 3 illustrates typical data input for *serac()*. The file, as the other input data files, must be saved in a tab separated '.txt' format, with periods as decimal delimiters. Depth top (depth_min) and bottom (depth_max) represent the sampling interval of each sample. The ^{137}Cs, ^{241}Am, and density columns are optional, but the latter (density) is required for inventory calculations, CFCS mass depth calculations and the CRS model. Even if all depths were not analyzed for short-lived radionuclides, all depths and corresponding densities are emplaced in the input file, in order to avoid extrapolating density data (NA in Table 3), which could present different patterns in regard to different environmental systems. If density data is not available, the analysed depths are sufficient to compute the CFCS and CIC models.

The function *serac_input_formatting('MyCore')* can be used to help format the input file. To use it, place the raw input file (column names in first row, data starting from the second row) in the folder as described above. This function asks the user to identify columns, rename them, and replace the input data file automatically.

Table 2. Summary of the functions around *serac*, for a core named 'MyCore'.

Function	Use	Output
user_infos()	New users run this function once to enter professional details	A .txt file in the ~/Cores folder with user's metadata
core_metadata(name = 'MyCore')	Before running serac, but once a folder 'MyCore' had been created in the ~/Cores folder, this function questions the user on metadata specifically related to the core (see Table 5 for details)	A serac_metadata_suppmetadata.txt file in the ~/Cores/MyCore folder This supplementary data will be included to the general metadata after each model computation.
serac_input_formatting(name = 'MyCore')	Input data file can be formatted outside R. This function can help correct several errors (columns names, unit for depth, density calculation, etc.)	Replace MyCore.txt in the ~/Cores/MyCore folder by a correctly formatted file and save the raw data in the same folder under the name MyCore_raw.txt
serac(name = 'MyCore', coring_year = 2019)	Main age-depth model computation function. Refer to Table 4 and case studies	Generate a plot in the ~/Cores/MyCore folder (if *plotpdf=TRUE*), a metadata file, and depth-age correspondence (raw and interpolated, according to resolution chosen by the *stepout* argument) for each type of model selected in the *model* argument.
serac_map()	*Function not describe in this paper – if GPS coordinates are given for the different cores (through the core_metadata() function), serac_map() will generate a map with the location of the different sites around the world*	A world map with the location of the different study sites

Table 3. *serac* input file for an example (Lake Iseo). Units are given as an indication, but should not be included in the input file to prevent any issues with file reading. * indicates input data that are optional. NA correspond to missing data: we recommend including continuous density data as $^{210}Pb_{ex}$ can be interpolated (or depth not considered) if needed, while density cannot.

depth_min (mm)	depth_max (mm)	density* (g/cm3)	Pb210ex (Bq/kg)	Pbex210_er (Bq/kg)	Cs137* (Bq/kg)	Cs137_er* (Bq/kg)	Am241* (Bq/kg)	Am241_er* (Bq/kg)
0	6	0.059	370	8	18.1	0.5	0.6	0.3
6	11	0.042	414	11	25.5	0.8	0.2	0.4
11	17	0.048	381	9	26.9	0.7	0.3	0.3
17	22.5	0.065	322	11	29.9	0.8	0.2	0.35

22.5	27.5	0.074	284	7	43.7	0.8	0.6	0.3
27.5	40.5	0.063	247.5	NA	NA	NA	NA	NA
40.5	48	0.052	211	8	77.5	1	0	0
48	54	0.053	249.5	NA	NA	NA	NA	NA
54	58.5	0.054	288	9	233	1.9	0.4	0.35
58.5	64.5	0.055	232	8	631	2.7	0.27	0.4
64.5	70.5	0.069	225	NA	NA	NA	NA	NA
70.5	75	0.082	218	9	1305	5	3.307	0.7
75	83	0.055	166	6	67.1	1	0.1	0.3
83	88.5	0.079	143	NA	NA	NA	NA	NA
88.5	95	0.065	120	6	38.4	0.6	0.7	0.25
95	101	0.057	139	NA	NA	NA	NA	NA
101	111	0.048	158	7	26.7	0.6	0.26	0.26
111	119	0.049	156	NA	NA	NA	NA	NA
119	130	0.050	154	6	47.9	0.8	1.2	0.3
130	139.5	0.072	129	6	155.6	1.5	3.79	0.4
139.5	150	0.087	88	5	96	0.9	1.09	0.29
150	159.5	0.101	96	6	61.6	1	1.1	0.4
159.5	164	0.107	82	6	19.1	0.4	0.55	0.28
164	173	0.097	63	6	7.7	0.3	0.14	0.3
173	179.5	0.107	55.5	NA	NA	NA	NA	NA
179.5	187.5	0.117	48	5	2.4	0.2	0.3	0.3
187.5	199.5	0.107	47	NA	NA	NA	NA	NA
199.5	209	0.106	46	3	0.7	0.1	0.2	0.16
209	234	0.107	40	NA	NA	NA	NA	NA
234	244.5	0.108	34	5	0.5	0.1	0	0
244.5	254	0.107	34	NA	NA	NA	NA	NA
254	264	0.105	34	5	0.23	0.14	0	0
264	283.5	0.108	31	NA	NA	NA	NA	NA
283.5	295	0.110	28	3	0.7	0.1	0	0
295	305	0.110	23	NA	NA	NA	NA	NA
305	317	0.109	18	4	0.19	0.13	0	0

On the next step, the user can then choose to compute age depth model(s) using any or all of the sedimentation hypotheses described in the previous section (CIC, CFCS, CRS, and CRS_pw). Note that the only requested arguments in the *serac()* function are the name of the core (must be the same than the folder and data input file names) and the coring year. All other arguments have default values and do not have to be filled on the first run. Some arguments are logical (i.e., TRUE or FALSE), other are entered in the form of vectors (e.g., list of sedimentation hypotheses, upper and lower limits for instantaneous deposits). All argument related to depth (e.g., depth of the Chernobyl peak) must be entered in millimetres. Table 4 summarises the main options, and the case studies included in the next section showcase different scenarios. A 'cheat sheet' summarising the steps and main functions is available in Supplementary Materials 1.

Table 4. Main options included in *serac*. Refer to Supplementary Material 2 for complete list of functions.

Category	Description
Site ID	**Only two arguments are mandatory to run the code: the name of the core and the coring year. Other arguments have default values that can be used**. The name of the core has to match the folder name and the file name with the input data.
$^{210}Pb_{ex}$	The user can choose to plot $^{210}Pb_{ex}$ measurements, with or without potential instantaneous deposits. One of the three models can be visualised. The choice to include or not include instantaneous deposits will automatically remove the corresponding measurements.
^{137}Cs	The user can choose to plot ^{137}Cs, and if so, to identify Chernobyl, the fallouts from nuclear war tests, and the firsts fallouts (logical arguments).
^{241}Am	The user can choose to plot ^{241}Am and identify the fallouts from nuclear war tests
Model	List of model(s) the user wants to test. Choice among CFCS, CRS, CIC, CRS_pw.
Photo	A photo of the sediment sequence can be added, upon precision of the upper and lower limit of the core (in mm). The photo will be automatically cropped.
Instantaneous deposit	Instantaneous deposits (flood, earthquake, slump layers) that should be excised can be added with this argument.
Ignore	For several reason, the user may want to ignore a measurement that is not part of an instantaneous deposit. This can be managed with this argument.
Sedimentation change	Up to two changes in the sedimentation rate can be tested. The depths of the changes are added in a vector.
Plot options	The user can choose whether to export the age-depth model figure using logical arguments. Colours and character size can also be modified.
Historic events	Historical events (e.g., flood, construction of a dam…) can be plotted on the last window.
Supplementary descriptor(s)	Up to two supplementary descriptors can be plotted. If done, an additional input file with these data should be included in the working folder.
Varves	Varve counting can be added on the age-depth model plot. If done, an additional input file with depths (in mm) and corresponding years must be included in the working folder.
Surface Mixed Layer	A depth in mm above which the sediment is considered to be mixed.
Mass depth	Logical (TRUE/FALSE) argument, to decide whether radionuclides should be plotted against mass accumulated depth. Default entries for sediment changes ignore instantaneous deposits and surface mixed layers, are in mm. Another argument (input_depth_mm) allows these depths to be entered in $g.cm^{-2}$ when turned to FALSE.

4. Case studies

4.1.Lake Bourget – A classic situation with one model (CFCS), one instantaneous event, and varves counting available

Lake Bourget (45°44.7420N, 5°51.6850E) is an 18 km long and 2.8 km wide lowland hard-water lake in the Northern French Alps. This core was sampled in the deepest part of the lake at 145 m water depth and records the recent eutrophication (Giguet-Covex et al., 2010). We used the CFCS model, identified one instantaneous deposit layer between 197 and 210 mm, and calculated a sediment accumulation rate SAR = 4.09 +/- 0.17 $mm.y^{-1}$. Varve counting being available since the appearance of hypoxia (Jenny et al., 2013), we requested these ages to be added to the output figure (*historic_d=c(197,210)*). We further identified dates from the nuclear war tests (first fallouts (220-230 mm), peak fallout (172-180 mm)), as well as traces of the Chernobyl accident (75-85 mm). In this example, we requested the output file to be produced at a 1 mm resolution (*stepout = 1*), and that the known earthquake of 1958 be visualized (*historic_d, historic_a, historic_n*, for depth, age, and name of the event). The full code is:

```
serac(name = "LDB", coring_yr = 2004, model = c("CFCS"), plotphoto = TRUE, minphoto =
c(0), maxphoto = c(370), plot_Pb = T, plot_Pb_inst_deposit = T, plot_Cs = T, plot_Am = T,
Cher = c(75, 85), Hemisphere = c("NH"), NWT = c(172, 180), FF = c(220, 230), inst_deposit =
c(197, 210), historic_d = c(197, 210), historic_a = c(1958), historic_n = c("earthquake 1958"),
varves = T, plotpdf = T, stepout = 1)
```

The high r^2 and the good adequation between ^{137}Cs and ^{241}Am, and historical ages, suggest the CFCS model is a good solution for this sediment core. More details on the several arguments are available in Supplementary Material 1.

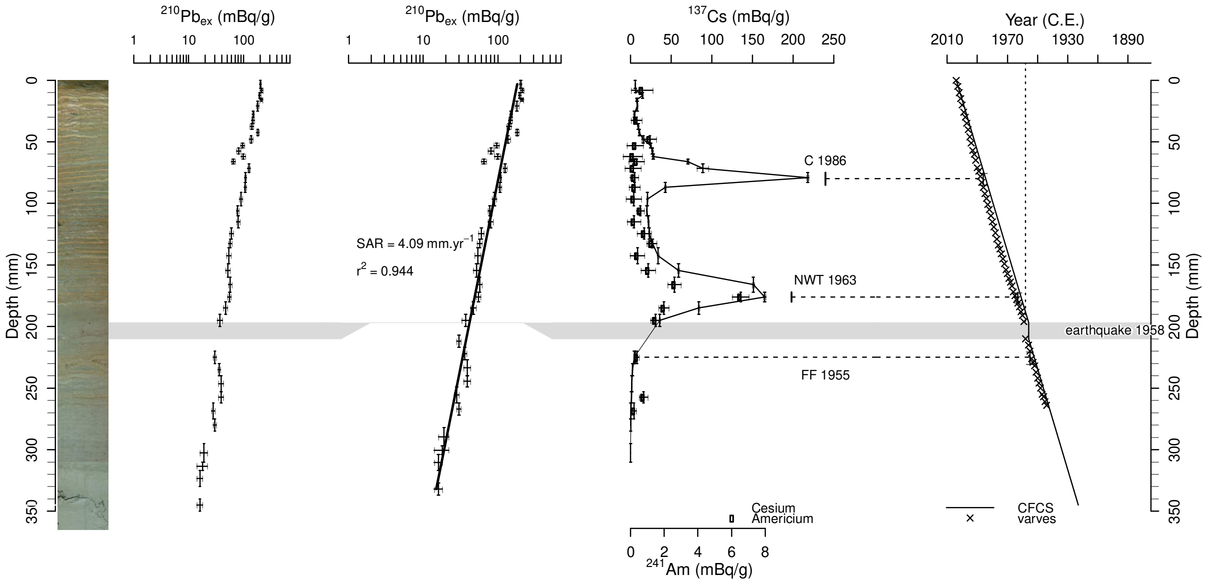

Figure 2. Short-lived radionuclides measurements, and age-depth model for Lake Bourget sediment core. From left to right: core photo, $^{210}Pbex$, $^{210}Pbex$ corrected of instantaneous deposits, ^{137}Cs and ^{241}Am activities and the CFCS age model with varve counting, ^{137}Cs and ^{241}Am peaks and the identification of the 1958 earthquake

4.2.Lake Iseo – An example of a sediment sequence where the three sedimentation hypotheses could be tested. Varve counting is also available.

Lake Iseo (45°44.205'N; 10°4.340'E) is a large lowland lake in Northern Italy 25 km long and 60.9 km² in surface area. This core is a sample from the Monte Isola plateau at approximately 70 m depth and contains evidence for a recent eutrophication (Rapuc et al., 2018). From short-lived radionuclides data on this core (Table 3), we calculated SAR = 3.16 mm.y^{-1}. In the script below, note that we request to visualise all three $^{210}Pb_{ex}$ models, ^{137}Cs

and ^{241}Am peaks and varve counting (Fig. 3), and used a 5 mm resolution for our interpolated model.

```
serac(name = "Iseo", coring_yr = 2010, model = c("CFCS", "CIC", "CRS"), plotphoto = TRUE,
minphoto = c(0), maxphoto = c(320), plot_Pb = T, plot_Am = T, plot_Cs = T, Cher = c(70, 75),
Hemisphere = c("NH"), NWT = c(130, 140), FF = c(164, 173), varves = TRUE, plotpdf = T,
stepout = 5)
```

The comparison between varve counting, artificial radionuclides and the ^{210}Pbex model shows that the CFCS model is preferable for this core and that there is evidence for the "too-old" age error described first by Binford (1990) for the CRS model in the deeper core sections and now widely observed (Abril, 2019; Tylmann et al., 2016, 2013). The "too-old" age error arises from an underestimation of ^{210}Pbex in deeper core sections in relation to analytical limitations, sampling strategy or both.

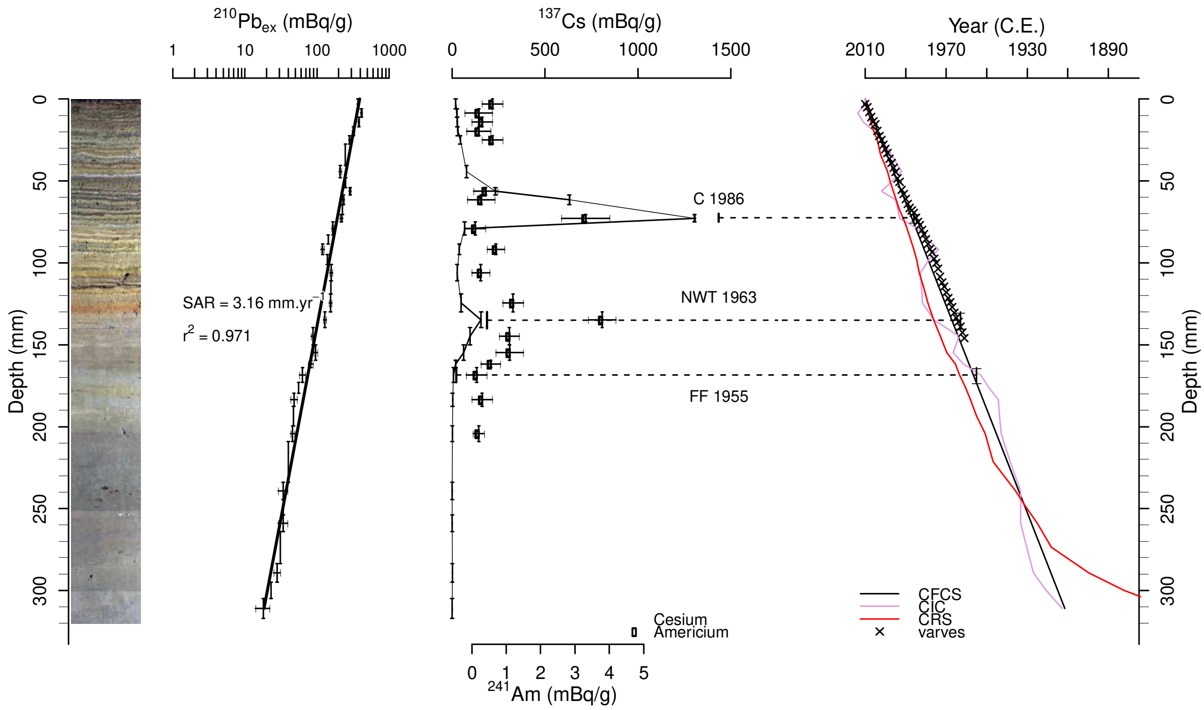

Figure 3. Short-lived radionuclides measurements, and age-depth model for Lake Iseo sediment core. From left to right: core photo, $^{210}Pb_{ex}$, ^{137}Cs and ^{241}Am activities and age model (CFCS, CIC, CRS) with varve counting and ^{137}Cs and ^{241}Am peaks.

4.3.Lake Luitel – an example of sediment sequence plot versus mass depth

Lake Luitel (FR) is a very small system (1.94 ha) located 1262 m above sea level, in a depression within the crystalline Belledonne range bedrock (Western Alps). The lake colour is black, typical of organic rich water and is encircled by bog type vegetation. An 80-cm-long core (LUI12P1) was collected from the deeper part of the lake (6 m) in 2012 to reconstruct the history of multiple industrial and urban mercury (Hg) emissions (Guédron et al., 2016).

This lake is rich in organic matter and thus presents a large amount of poral water; the classic CFCS model does not match the ^{137}Cs fallouts well (note that ^{241}Am was under the detection limit and is thus not presented in Fig. 4). In such a lake system, a semilogarithmic plot of $^{210}Pb_{ex}$ activities versus mass depth allows us to consider density variations in regard to sediment compaction (Abril, 2019; Tylmann et al., 2016). We thus present the CRS, CRS_pw and CFCS models based on the mass depth model (Fig. 4). The CIC model displays several ages inversions, which we want to avoid, and is not shown here. For the CFCS model, the MAR is well defined (0.047 $g.mm^{-1}.y^{-1}$, r^2= 0.975) and the age model is in good agreement with the 1955 and 1963 AD ^{137}Cs markers and in a lesser extent with the Chernobyl fallout, although better than CFCS based on depth age model (not shown). The CRS model also provides a good age model in regard to the ^{137}Cs data, but still present too old ages for the deeper samples. The CRS_pw model is by definition in good agreement with ^{137}Cs markers as we use 1986, 1963 and 1955 AD as forced time-markers (Fig. 4). Therefore, CRS_pw model is better than the CFCS one for the upper part of the core until ~350 mm. Below 350 mm, similar to the CRS model, CRS_pw presents too old ages. For the deeper part of the core as no sedimentary variation is observed it is better to use the mass depth CFCS model which do not present large MAR variation. The best age modelling is done thanks to *serac* and includes the CFCS or CRS_pw mass depth calculation with the following arguments:

```
serac(name = "LUI", coring_yr = 2012, model = c("CFCS", "CRS", "CRS_pw"), mass_depth =
T, plotphoto = T, minphoto = c(0), maxphoto = c(470), plot_Pb = T, plot_Cs = T, Cher = c(115,
125), Hemisphere = c("NH"), NWT = c(285, 295), FF = c(305, 315), plotpdf = TRUE,
depth_forced_CRS = c(115, 285, 305), age_forced_CRS = c(1986, 1963, 1955))
```

Note that the ^{137}Cs peaks (or other depth-related arguments) were identified in the *serac* function in mm (the default), but could also be entered in $g.cm^{-2}$ by adding the argument *input_depth_mm = F*.

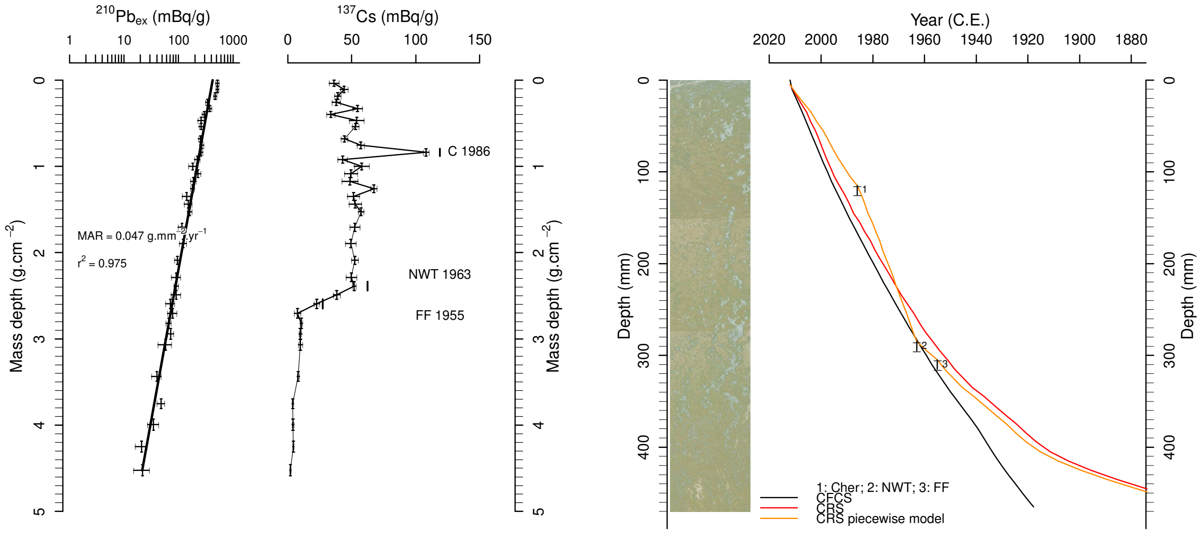

Figure 4. Short-lived radionuclides measurements, and age-depth model for Lake Luitel sediment core. From left to right: ^{210}Pbex activities, ^{137}Cs activities, photo of the core, and the age models (CFCS_mass_depth, CRS and CRS_pw). Note that in the left and central parts, data are plotted against mass depth, while in the right part, data are plotted against depth.

4.4. Lake Saint André – an example of sediment sequence with changes in the sedimentation rate

Lake Saint André (FR) is a relatively small system (7.64 ha), formed in 1248 after a large landside. Vineyards have occupied approximately 36% of its 48.5 ha watershed since the beginning of World War II. A 1-m core (SAN11P2) was collected from the deepest part of Lake Saint André (12 m) in 2011 to investigate long-term succession and the diffuse transfer of herbicides, fungicides, and insecticide treatments (Sabatier et al., 2014).

A logarithmic plot of $^{210}Pb_{ex}$ activity (Fig. 5) shows a general decrease with three distinct linear trends. According to the (CFCS) model applied to each part of the profile, we can define mean accumulation rates of 2.9 ± 0.2 mm.y^{-1} between depths of 41 and 26 cm, 5.3 ± 0.6 mm.y^{-1} between 26 and 16.5 cm, and 8.6 ± 1.3 mm.y^{-1} in the upper 16.5 cm of the core. ^{137}Cs and ^{241}Am activities are in good agreement with the ages derived from the $^{210}Pb_{ex}$-CFCS model and support the interpretation of two primary sedimentation rate changes in ca. 1973 ± 5 y and 1994 ± 2.5 y (Fig. 5). These two changes in the sedimentation rate are related to vineyard practices increasing erosion in the watershed during two periods: (1) in the early 1970s, with the local use of heavy farm machinery and (2) in the early 1990s, with increasing applications of postemergence herbicides (Glyphosate, see Sabatier et al., 2014 for more details). The age modelling conducted through *serac,* including the two changes in sedimentation rate, takes the following arguments:

```
serac(name = "SAN", coring_yr = 2011, model = c("CFCS", "CIC", "CRS", "CRS_pw"), plotphoto = TRUE, minphoto = c(0), maxphoto = c(420), plot_Pb = T, sedchange = c(165, 260), plot_Am = T, plot_Cs = T, Cher = c(195, 205), Hemisphere = c("NH"), NWT = c(285, 295), FF = c(315, 325), plotpdf = TRUE, depth_forced_CRS = c(200, 290, 320), age_forced_CRS = c(1986, 1963, 1955), archive_metadata = T)
```

The piecewise CFCS and CRS_pw models are in best agreement with ^{137}Cs/^{241}Am markers. CRS_pw models with 3 forced depths seems good until 350 mm and deeper present large chronology deviation but provide more smoothed SAR changes than CFCS model. Knowing the environmental context of this lake system with 2 strong changes in agricultural practices we expect a rapid change in SAR derived from rapid change in erosional processes and thus we prefer the piecewise CFCS model (Sabatier et al., 2014).

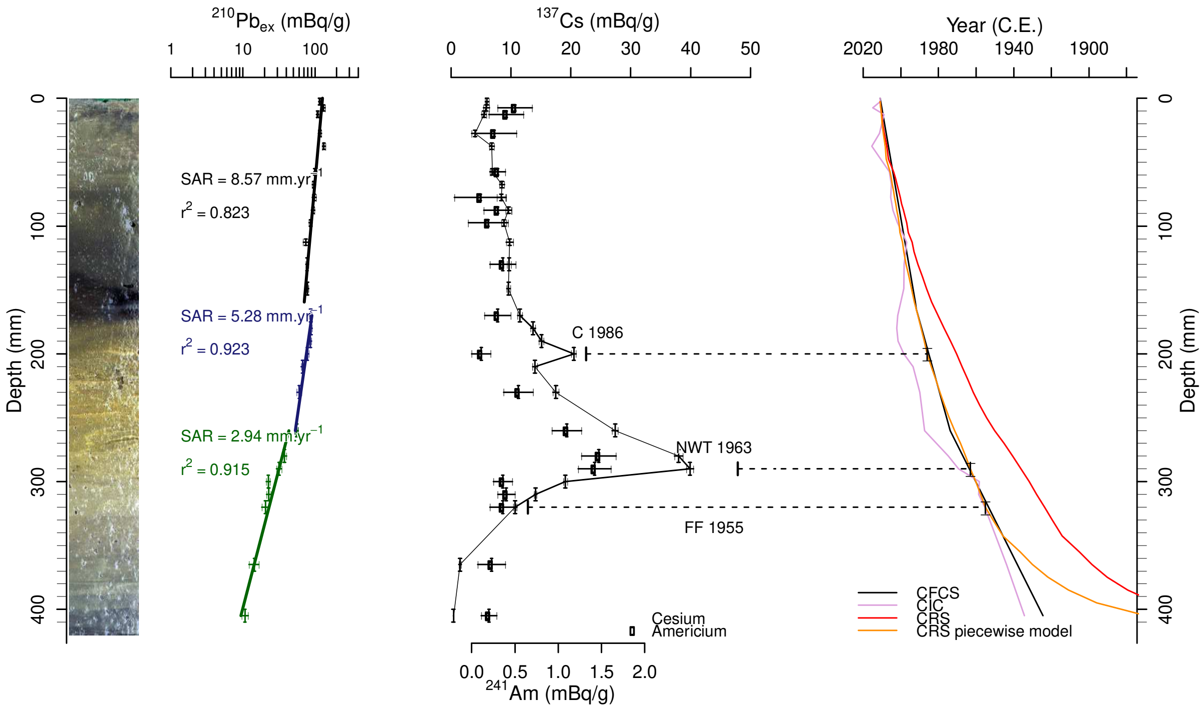

Figure 5. Short-lived radionuclides measurements, and age-depth model for Lake Saint André sediment core. From left to right: photography, $^{210}Pbex$ activity, ^{137}Cs and ^{241}Am activities, and the age model (CFCS, CRS, CIC and CRS_pw).

4.5.Lake Allos – an example of a sediment sequence with instantaneous deposits

Lake Allos is a high-altitude lake in the French Alps (2230 m a.s.l., 0.6 km^2). Half of the 5-km^2 catchment is drained by three permanent torrents that transport terrigenous flows towards the lake mainly during extreme precipitation events (Wilhelm et al., 2015, 2012). A plot of $^{210}Pb_{ex}$ activity (Fig. 6) shows a general decrease with low activities at several depths that correspond to graded beds. To illustrate these sedimentary events, we add one to two supplementary descriptors (*suppdescriptor*) to the age model figure, such as geochemical data (XRF). Calcium (*Ca*) enrichment associated with coarser grain size evidence four instantaneous deposits in the Allos sediment sequence, indicating a large input from the watershed, while iron (*Fe*) content is associated with continuous sedimentation (Fig. 6, see Wilhelm et al., 2012 for more details). As these instantaneous events are removed before computing the CFCS model, which assumes a linear sedimentation rate. In this case, $^{210}Pb_{ex}$ activities, corrected for instantaneous deposits, show a change in the mean sedimentation rate at 71 mm. CRS and CRS_pw models were also computed without all these instantaneous events and provide very similar results than piecewise CFCS model. The age modelling is conducted through *serac* and includes the historical events and one change in sedimentation rate with the following arguments:

```
serac(name = "ALO09P12", coring_yr = 2009, model = c("CFCS", "CRS","CRS_pw"),
plotphoto = TRUE, minphoto = c(0), maxphoto = c(210), plot_Pb = T, plot_Pb_inst_deposit =
T, inst_deposit = c(20, 28, 100, 107, 135, 142, 158, 186), sedchange = c(71), plot_Am = T,
plot_Cs = T, Cher = c(35, 40), Hemisphere = c("NH"), NWT = c(51, 61), suppdescriptor =
TRUE, descriptor_lab = c("Ca (cps)", "Fe (cps)"), historic_d = c(20, 28, 100, 107, 135, 142,
158, 186), historic_a = c(1994, 1920, 1886, 1868), historic_n = c("sept 1994 flood", "1920
flood", "1886 flood", "1868 flood ?"), min_yr = c(1750), dmax = c(180), plotpdf = TRUE,
depth_forced_CRS = c(37.5,58.5), age_forced_CRS = c(1986, 1963))
```

The final age model is supported by the ^{137}Cs and ^{241}Am activities and by historical floods that correspond to these four instantaneous events. Note that for larges figures as Fig. 6, R may sometimes not create the preview (and gives an error) because the plotting window is too narrow. The user can try to extend the plotting zone (which is easy in RStudio, RStudio Team, 2016). We added a logical argument, *preview*, which can be turned to FALSE to address this issue; in this case, the preview is simply not displayed. If the argument *plotpdf* is left to its default value, i.e., TRUE, the figure will still be created in the core subfolder.

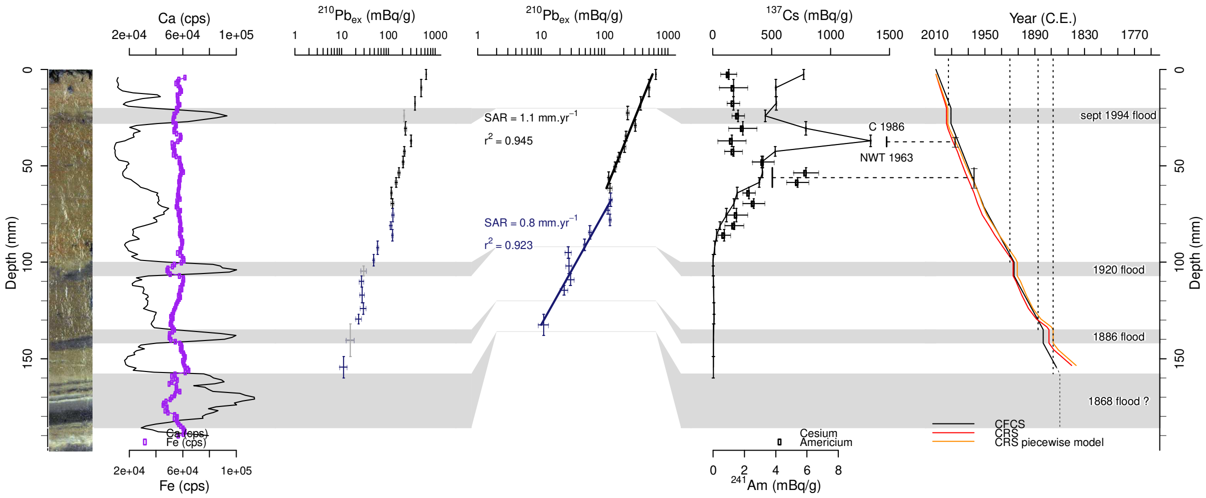

Figure 6. Descriptors, short-lived radionuclides measures, and age-depth model for Lake Allos sequence. From left to right: core photograph, Ca/Fe ratio and raw Fe, $^{210}Pb_{ex}$ activity with and without instantaneous deposit events, ^{137}Cs activity and ^{241}Am activity, and the CFCS, CRS and CRS_pw age model for the Lake Allos sequence. The horizontal grey lines indicate layers that were identified as instantaneous events.

4.6. Pierre Blanche lagoon – An example of a sediment sequence with a surface mixed layer

The PB06 core (7.9 m) was collected in the Pierre Blanche Lagoon (PBL), in the southern part of the Palavasian lagoonal complex (France) in 2006 (Sabatier et al., 2010b). This coastal shallow water environment contains many organisms that induce bioturbation, with advection-diffusion in the upper first centimetres in the deepest regions caused by mollusc and gallery-diffusion by worms (François et al., 2002). This second process is difficult to identify and to correct for (Sabatier et al., 2010a). The resolution of the advection-diffusion model (Sharma et al., 1987) by Lecroart *et al.* (2007) applied to $^{210}Pb_{ex}$ allows the estimation of SARs and the biodiffusion coefficient (D_b). We can thus define a surface mixed layer (SML) within which $^{210}Pb_{ex}$ activities are perturbed; PB06 has almost constant activities in the first 3 cm (Fig. 7). The $^{210}Pb_{ex}$ activities profile is thus composed of a bioturbated upper part, characterised by a combination of sedimentation and bioturbation (SAR, D_b) and below which a non-perturbed profile exists where D_b= 0. To solve this model, we calculated a mean sedimentation rate for the non-bioturbated part and, making the hypothesis the sedimentation rate remained constant, we extrapolated this estimate to the upper part. The SML is defined in *serac* by its upper and lower depth. In the presence of SML, CIC model cannot be applied because the initial activity is perturbed. The age model for PB06 is also constrained by the ^{137}Cs peaks and a historical storm event identified by geochemical data (Fig. 7); for more details see Sabatier et al. (2010c). The full *serac* code is:

```
serac(name = "PB06", coring_yr = 2006, model = c("CFCS", "CRS", "CRS_pw"), plotphoto =
TRUE, minphoto = c(0), maxphoto = c(350), plot_Pb = T, plot_Pb_inst_deposit = T,
```

```
inst_deposit = c(315, 350), SML = 30, plot_Cs = T, Cher = c(50, 60), Hemisphere = c("NH"),
NWT = c(100, 120), suppdescriptor = T, descriptor_lab = c("Si/Al"), historic_d = c(315, 350),
historic_a = c(1893), historic_n = c("1894 storm"), min_yr = 1870, dmax = c(350), plotpdf =
TRUE, depth_forced_CRS = c(55, 105), age_forced_CRS = c(1986, 1963))
```

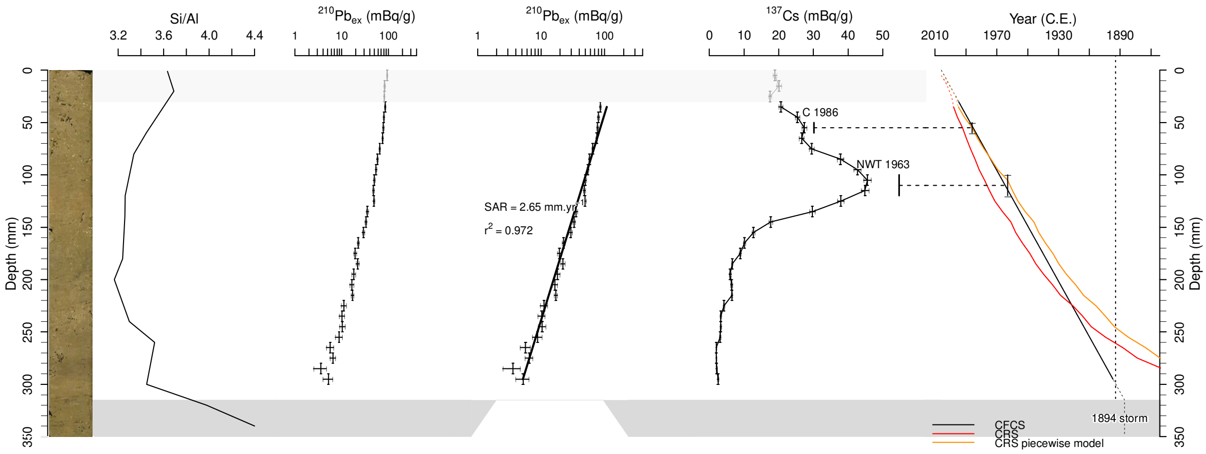

Figure 7. Descriptor, short-lived radionuclides measurements, and age-depth model for Pierre-Blanche lagoon sediment core. From left to right: core photograph, Si/Al content, $^{210}Pb_{ex}$ activities, ^{137}Cs activities, and the age model (CFCS, CRS and CRS_pw), the surface mixed layer is in light grey and the 1894 AD storm event in dark grey.

The comparison among historical events (storms), artificial radionuclides and the $^{210}Pb_{ex}$ model results in the CFCS model being preferable to the CRS and CRS_pw for this core and evidence of the "too-old" age error described by Binford (1990) for the CRS models in the deeper core sections, resulting from the identified 1894 storm event.

5. Metadata

Every time the code is run, a metadata file is automatically generated in the folder. The metadata file summarises the main decisions made by the user (e.g., presence/absence of instantaneous deposit, type of model chosen) but also other general information on the user (ORCID, affiliation, email) and the core (ISGN: International Geo Sample Number (IGSN)/System for Earth Sample Registration Database (www.geosamples.org, measurement laboratory, measurement method, date of measurement). These data are entered independently from the exploration phase of the model through the function user_infos() and core_metadata(). The former function theoretically needs to be used only once by each new user the first time the library *serac* is used. The new user will be required to answer several questions (affiliation, ORCID number, etc.). The user information are then integrated into the metadata file associated with the age modelling, in text format. The core_metadata() function ask more details about the core itself and the analytical data, summarised in Table 4 and will be enter according to the following lines:

```
core_metadata(name = "Mycore")
```

These data can also be directly implemented during the age modelling phase by adding archive_metadata=T in the *serac* function. The metadata listed in Table 5 emerges from both data reports of radioactivity detections from the CNRS in France (Centre National de la Recherche Scientifique) and a recent international survey (literature review and questionnaire) about ^{210}Pb metadata (Courtney Mustaphi et al., 2019). The French initiative coordinated the development of a common way to present short-lived radionuclides data through the ROZA (Rétro-observatoire Archives sédimentaires des Zones Ateliers) experience and produced a document guiding the information needed to store data in a repository. The review by Courtney Mustaphi et al. (2019) also suggests a set of minimum reporting guidelines for ^{210}Pb metadata and data needed to improve data archiving standards to facilitate data reutilisation.

Table 5. Example of metadata associated with the SAN core (Sabatier et al., 2014)

Parameters	Example
ISGN	EDYSAN001
sample date	2011-12-01
coring coordinates y	45.494980
coring coordinates x	5.985720
coring method	gravity corer
laboratory subsampling method	calibrated volumetric sampler
measurement laboratory	LSM/EDYTEM, FR
instrument type	well-type germanium detector
measurement startdate	2012-01-15
measurement enddate	2012-04-05
additional comments	^{210}Pb background reached

These two functions and all parameters inside are optional but we encourage the users to use these functionalities as they help generate a more exhaustive background for the core. Note that another text file is automatically generated and incremented with all new tests. The file is found in the core folder (~/Cores/MyCore/serac_model_history_MyCore.txt). It (1) provides a history of attempts and (2) displays a message in R if a code has been tested previously. A vigilant user can then compare and trace back the logical thinking that led to the final model.

6. Discussion

serac provides a rapid yet exhaustive tool for testing sedimentation hypotheses and creating age models for the last century. Several functions (Table 2) guide the user in building age-depth models for a given core. To choose the best chronology for the studied sequence, *serac* allows the comparison of different age models to be computed against depth or mass depth, but also to be compared with other independent markers such as artificial radionuclides fallout or historic events. In most cases, we recommend users to plot ^{210}Pbex activities versus mass depth as this representation take into account both natural and coring compactions which remain invariant under the previous processes (Fig. 4). Note that the identification of independent time marker such as artificial radionuclides (Fig. 2-6) or historical events (Fig. 2, 5, 6) is often necessary to validate the age model choice (Baskaran et al., 2014; Kirchner, 2011). However, users have to be aware of potential wrong identification of i) the first ^{137}Cs atmospheric fallout when non-ideal deposition is relevant with diffusion (Delaval et al., 2020) or mixing (Sabatier et al., 2010a) and ii) ^{137}Cs-peaks when translocational and/or incomplete mixing occur (Abril, 2004; Sabatier et al., 2010a).

$^{210}Pb_{ex}$ models are sometime used incorrectly. For instance, CIC model cannot be used for a core that has instantaneous deposits with lower $^{210}Pb_{ex}$ activities or a surface mixed layer linked to bioturbation processes. Furthermore, the CRS model cannot be used when the $^{210}Pb_{ex}$ inventory is not the total (activities were not measured until secular equilibrium existed between ^{210}Pb and ^{226}Ra). Note that *serac* will display warnings when sedimentation hypotheses are not satisfied. In that respect, *serac* is also a pedagogic tool.

Other parameters non-related to sedimentation hypotheses are automatically computed in *serac*. If the density is present in the input data, ^{210}Pb and ^{137}Cs inventories of sediment cores are generated. These data can be interesting to compare across systems to map the trajectory of radionuclide fallouts. For instance, ^{137}Cs inventories of Lake Iseo (1390 ± 100 $Bq.m^{-2}$) and Lake Bourget (975 ± 19 $Bq.m^{-2}$) reported the same age of 2020, but present significant differences related to the higher Chernobyl accident fallout in Italy relative to that in France. Inventories can also indicate allochthonous inputs variations, and comparisons across sites can yield valuable insights into catchment sediment dynamics (Pulley et al., 2018). Finally, radionuclides inventories of multiples cores in different part of the same lake allow to identify sediment redistribution from shallow to deep zone by waves and water currents through sediment focusing (Crusius and Anderson, 1995).

Using *serac* easily allows reproducibility of the main hypotheses behind any age-depth model (such as changes in sedimentation rates or the presence of instantaneous deposits). We believe that the availability of a user-friendly code on an open source platform to visualise and test sedimentation hypotheses is an important step towards reproducibility. *serac* allows users customisation of parameters to include, as well as cross-platform support (Windows, Linux, Macs). The R code of *serac* can be understood relatively easily by a beginner R user, and its open source nature means it can be adapted to fit an advanced user's preferences. Output files (age model, metadata, figure) could be used (1) in the current form or integrated in a larger age model such as *clam* (2) to create a figure for publication and (3) in data saving platforms with general information on data, metadata, the age modeller, and the age model parameters, which would allow data tractability and reproducibility. It is hoped that *serac* could help the palaeoscience community standardise and enhance future age depth models that use sort-lived radionuclides and allow the extension of the data lifecycle (Wilkinson et al., 2016).

7. Conclusion

The past century is characterized by rapid environmental socio-ecological changes, as showcased by the few case studies we presented before (e.g., Sabatier et al., 2014). Consequences of environmental modifications and critical ecosystem thresholds can be informed resorting to historical reconstructions. Shortlived radionuclides are essential for developing ages models for the past 100 years and setting a convincing chronology for changes unveiled by proxies.

serac complement other tools by offering a method to produce age-depth model using radionuclides data with classic model applications (CFCS, CIC, CRS) and piecewise versions. The automation allows to try different sedimentation hypothesis, makes unlikely calculation errors and saves computational time that can now be allocated to comparing different chronological models or further analyses.

An important feature of *serac* is the generation of metadata. Good report of metadata relative to the core or the model is not common yet (Courtney Mustaphi et al., 2019), but is decisive to extend the data life cycle and promote knowledge integration by the community (Courtney Mustaphi et al., 2019; Wilkinson et al., 2016).

Acknowledgements

We thank A.-L. Develle and W. Rapuc for beta testing previous versions of *serac* and C. Pignol for recommendations on metadata outputs through the ROZA (Rétro-observatoire Archives sédimentaires des Zones Ateliers) experience at the CNRS (Centre National de

Recherche Scientifique français). We thank Dr. Bollhoefer (associate editor) and two anonymous reviewers for their comments and suggestions that improved the paper.

Data Availability

Data to reproduce the example for Lake Allos (Fig. 6) are accessible through the package. Other data are available upon request.

References

Abril Hernández, J.-M., 2016. A 210 Pb-based chronological model for recent sediments with random entries of mass and activities: Model development. J. Environ. Radioact. 151, 64–74. https://doi.org/10.1016/j.jenvrad.2015.09.018

Abril, J.M., 2020. Multimodal-TERESA, a 210Pb-based radiometric dating model for recent sediments under largely varying rates of supply. Quat. Geochronol. 55, 101032. https://doi.org/10.1016/j.quageo.2019.101032

Abril, J.M., 2019. Radiometric dating of recent sediments: On the performance of 210Pb-based CRS chronologies under varying rates of supply. Quaternary Geochronology 51, 1–14. https://doi.org/10.1016/j.quageo.2018.12.003

Abril, J.M., 2004. Constraints on the use of 137Cs as a time-marker to support CRS and SIT chronologies. Environ. Pollut. 129, 31–37. https://doi.org/10.1016/j.envpol.2003.10.004

Abril, J.-M., Gharbi, F., 2012. Radiometric dating of recent sediments: beyond the boundary conditions. J. Paleolimnol. 48, 449–460. https://doi.org/10.1007/s10933-012-9622-5

Andrews, A., Stone, R., Lundstrom, C., DeVogelaere, A., 2009. Growth rate and age determination of bamboo corals from the northeastern Pacific Ocean using refined 210Pb dating. Marine Ecology Progress Series 397, 173–185. https://doi.org/10.3354/meps08193

Appleby, P.G., 2008. Three decades of dating recent sediments by fallout radionuclides: a review. The Holocene 18, 83–93. https://doi.org/10.1177/0959683607085598

Appleby, P.G., 2001. Chronostratigraphic Techniques in Recent Sediments, in: Last, W.M., Smol, J.P. (Eds.), Tracking Environmental Change Using Lake Sediments, Basin Analysis, Coring, and Chronological Techniques. Developments in Paleoenvironmental Research Series. Dordrecht, pp. 171–203.

Appleby, P.G., Oldfield, F., 1992. Applications of lead-210 to sedimentation studies, in: Uranium-Series Disequilibrium: Applications to Earth, Marine, and Environmental Sciences. Clarendon Press ; Oxford University Press, Oxford : Oxford ; New York.

Appleby, P.G., Oldfield, F., 1978. The calculation of lead-210 dates assuming a constant rate of supply of unsupported ^{210}Pb to the sediment. CATENA 5, 1–8. https://doi.org/10.1016/S0341-8162(78)80002-2

Appleby, P.G., Richardson, N., Nolan, P.J., 1991. 241Am dating of lake sediments. Hydrobiologia 214, 35–42. https://doi.org/10.1007/BF00050929

Aquino-López, M.A., Blaauw, M., Christen, J.A., Sanderson, N.K., 2018. Bayesian Analysis of ^{210}Pb Dating. JABES 23, 317–333. https://doi.org/10.1007/s13253-018-0328-7

Arias-Ortiz, A., Masqué, P., Garcia-Orellana, J., Serrano, O., Mazarrasa, I., Marbà, N., Lovelock, C.E., Lavery, P., Duarte, C.M., 2018. Reviews and syntheses: ^{210}Pb-derived sediment and carbon accumulation rates in vegetated coastal ecosystems: setting the record straight. Biogeosciences Discussions 1–47. https://doi.org/10.5194/bg-2018-78

Baskaran, M., Iliffe, T.M., 1993. Age determination of recent cave deposits using excess ^{210}Pb - A new technique. Geophysical Research Letters 20, 603–606. https://doi.org/10.1029/93GL00531

Baskaran, M., Nix, J., Kuyper, C., Karunakara, N., 2014. Problems with the dating of sediment core using excess 210Pb in a freshwater system impacted by large scale watershed changes. J. Environ. Radioact 138, 355–363. https://doi.org/10.1016/j.jenvrad.2014.07.006

Binford, M.W., 1990. Calculation and uncertainty analysis of ^{210}Pb dates for PIRLA project lake sediment cores. J Paleolimnol 3, 253–267.

Blaauw, M., 2010. Methods and code for 'classical' age-modelling of radiocarbon sequences. Quat. Geochronol. 5, 512–518. https://doi.org/10.1016/j.quageo.2010.01.002

Blais, J.M., Kalff, J., Cornett, R.J., Evans, R.D., 1995. Evaluation of ^{210}Pb dating in lake sediments using stable Pb, Ambrosia pollen, and ^{137}Cs. J. Paleolimnol. 13, 169–178.

Carroll, J., Lerche, I., 2003. Sedimentary processes: quantification using radionuclides. Elsevier, Amsterdam; Boston.

Condomines, M., Rihs, S., 2006. First 226Ra–210Pb dating of a young speleothem. Earth and Planetary Science Letters 250, 4–10. https://doi.org/10.1016/j.epsl.2006.06.012

Cooke, C.A., Hobbs, W.O., Michelutti, N., Wolfe, A.P., 2010. Reliance on ^{210} Pb Chronology Can Compromise the Inference of Preindustrial Hg Flux to Lake Sediments. Environmental Science & Technology 44, 1998–2003. https://doi.org/10.1021/es9027925

Courtney Mustaphi, C.J., Brahney, J., Aquino-López, M.A., Goring, S., Orton, K., Noronha, A., Czaplewski, J., Asena, Q., Paton, S.C., Panga Brushworth, J., 2019. Guidelines for reporting and archiving ^{210}Pb sediment chronologies to improve fidelity and extend data lifecycle. Quat. Geochronol. 52, 77–87.

Crusius, J., Anderson, R.F., 1995. Sediment focusing in six small lakes inferred from radionuclide profiles. J Paleolimnol 13, 143–155. https://doi.org/10.1007/BF00678103

Delaval, A., Duffa, C., Radakovitch, O., 2020. A review on cesium desorption at the freshwater-seawater interface. J. Environ. Radioact. 218, 106255. https://doi.org/10.1016/j.jenvrad.2020.106255

Druffel, E.R.M., King, L.L., Belastock, R.A., Buesseler, K.O., 1990. Growth rate of a deep-sea coral using 210Pb and other isotopes. Geochimica et Cosmochimica Acta 54, 1493–1499. https://doi.org/10.1016/0016-7037(90)90174-J

François, F., Gerino, M., Stora, G., Durbec, J.-P., Poggiale, J.-C., 2002. Functional approach to sediment reworking by gallery-forming macrobenthic organisms: modeling and application with the polychaete Nereis diversicolor. Mar. Ecol. Prog. Ser. 229, 127–136. https://doi.org/10.3354/meps229127

Giguet-Covex, C., Arnaud, F., Poulenard, J., Enters, D., Reyss, J.-L., Millet, L., Lazzaroto, J., Vidal, O., 2010. Sedimentological and geochemical records of past trophic state and hypolimnetic anoxia in large, hard-water Lake Bourget, French Alps. J. Paleolimnol. 43, 171–190. https://doi.org/10.1007/s10933-009-9324-9

Goldberg, E.D., 1963. Geochronology with 210 Pb in radioactive dating. International Atomic Energy Contribution 1510, 121–131.

Guédron, S., Amouroux, D., Sabatier, P., Desplanque, C., Develle, A.-L., Barre, J., Feng, C., Guiter, F., Arnaud, F., Reyss, J.L., Charlet, L., 2016. A hundred year record of industrial and urban development in French Alps combining Hg accumulation rates and isotope composition in sediment archives from Lake Luitel. Chemical Geology 431, 10–19. https://doi.org/10.1016/j.chemgeo.2016.03.016

Jenny, J.-P., Arnaud, F., Dorioz, J.-M., Giguet-Covex, C., Frossard, V., Sabatier, P., Millet, L., Reyss, J.-L., Tachikawa, K., Bard, E., Pignol, C., Soufi, F., Romeyer, O., Perga, M.-E., 2013. A spatiotemporal investigation of varved sediments highlights the dynamics of hypolimnetic hypoxia in a large hard-water lake over the last 150 years. Limnol. Oceanogr. 58, 1395–1408. https://doi.org/10.4319/lo.2013.58.4.1395

Kirchner, G., 2011. 210Pb as a tool for establishing sediment chronologies: examples of potentials and limitations of conventional dating models. J. Environ. Radioact, International Topical Meeting on Polonium and Radioactive Lead Isotopes 102, 490–494. https://doi.org/10.1016/j.jenvrad.2010.11.010

Krishnaswamy, S., Lal, D., Martin, J.M., Meybeck, M., 1971. Geochronology of lake sediments. Earth Planet. Sci. Lett. 11, 407–414. https://doi.org/10.1016/0012-821X(71)90202-0

Lecroart, P., Schmidt, S., Anschutz, P., Jouanneau, J.-M., 2007. Modeling sensitivity of biodiffusion coefficient to seasonal bioturbation. J. Mar. Res. 65, 417–440. https://doi.org/10.1357/002224007781567630

Moore, W.S., Krishnaswami, S., 1972. Coral growth rates using228Ra and210Pb. Earth and Planetary Science Letters 15, 187–190. https://doi.org/10.1016/0012-821X(72)90059-3

Pennington, W., Cambray, R.S., Eakins, J.D., Harkness, D.D., 1976. Radionuclide dating of the recent sediments of Blelham Tarn. Freshw. Biol. 6, 317–331. https://doi.org/10.1111/j.1365-2427.1976.tb01617.x

Pulley, S., Foster, I.D.L., Collins, A.L., Zhang, Y., Evans, J., 2018. An analysis of potential controls on long-term 137Cs accumulation in the sediments of UK lakes. J. Paleolimnol. 60, 1–30. https://doi.org/10.1007/s10933-017-0016-6

Putyrskaya, V., Klemt, E., Röllin, S., Corcho-Alvarado, J.A., Sahli, H., 2020. Dating of recent sediments from Lago Maggiore and Lago di Lugano (Switzerland/Italy) using ^{137}Cs and ^{210}Pb. Journal of Environmental Radioactivity 212, 106135. https://doi.org/10.1016/j.jenvrad.2019.106135

R Core Team, 2020. R: A language and environment for statistical computing. R Foundation for Statistical Computing, Vienna, Austria. R Foundation for Statistical Computing.

Rapuc, W., Sabatier, P., Andrič, M., Crouzet, C., Arnaud, F., Chapron, E., Šmuc, A., Develle, A.-L., Wilhelm, B., Demory, F., Reyss, J.-L., Régnier, E., Daut, G., Von Grafenstein, U., 2018. 6600 years of earthquake record in the Julian Alps (Lake Bohinj, Slovenia). Sedimentology 65, 1777–1799. https://doi.org/10.1111/sed.12446

Robbins, J., Krezoski, J., Mozley, S., 1977. Radioactivity in sediments of the Great Lakes: Post-depositional redistribution by deposit-feeding organisms. Earth Planet. Sci. Lett. 36, 325–333. https://doi.org/10.1016/0012-821X(77)90217-5

RStudio Team, 2016. RStudio: Integrated Development for R. RStudio, Inc., Boston, MA.

Sabatier, P., Dezileau, L., Barbier, M., Raynal, O., Lofi, J., Briqueu, L., Condomines, M., Bouchette, F., Certain, R., Grafenstein, U.V., Jorda, C., Blanchemanche, P., 2010a. Late-Holocene evolution of a coastal lagoon in the Gulf of Lions (South of France). Bulletin de la Société Géologique de France 181, 27–36. https://doi.org/10.2113/gssgfbull.181.1.27

Sabatier, P., Dezileau, L., Blanchemanche, P., Siani, G., Condomines, M., Bentaleb, I., Piquès, G., 2010b. Holocene Variations of Radiocarbon Reservoir Ages in a Mediterranean Lagoonal System. Radiocarbon 52, 91–102.

Sabatier, P., Dezileau, L., Briqueu, L., Colin, C., Siani, G., 2010c. Clay minerals and geochemistry record from northwest Mediterranean coastal lagoon sequence: Implications for paleostorm reconstruction. Sedimentary Geology 228, 205–217. https://doi.org/10.1016/j.sedgeo.2010.04.012

Sabatier, P., Poulenard, J., Fanget, B., Reyss, J.-L., Develle, A.-L., Wilhelm, B., Ployon, E., Pignol, C., Naffrechoux, E., Dorioz, J.-M., Montuelle, B., Arnaud, F., 2014. Long-term relationships among pesticide applications, mobility, and soil erosion in a vineyard watershed. Proc. Natl. Acad. Sci. 111, 15647–15652. https://doi.org/10.1073/pnas.1411512111

Sabatier, P., Reyss, J.-L., Hall-Spencer, J.M., Colin, C., Frank, N., Tisnérat-Laborde, N., Bordier, L., Douville, E., 2012. ²¹⁰Pb-²²⁶Ra chronology reveals rapid growth rate of <i>Madrepora oculata</i> and <i>Lophelia pertusa</i> on world's largest cold-water coral reef. Biogeosciences 9, 1253–1265. https://doi.org/10.5194/bg-9-1253-2012

Sanchez-Cabeza, J.A., Ruiz-Fernández, A.C., 2012. ^{210}Pb sediment radiochronology: An integrated formulation and classification of dating models. Geochim. Cosmochim. Acta, Environmental Records of Anthropogenic Impacts 82, 183–200. https://doi.org/10.1016/j.gca.2010.12.024

Sharma, P., Gardner, L.R., Moore, W.S., Bollinger, M.S., 1987. Sedimentation and bioturbation in a salt marsh as revealed by ^{210}Pb, ^{137}Cs, and ^{7}Be studies: Sedimentation and bioturbation. Limnol. Oceanogr. 32, 313–326. https://doi.org/10.4319/lo.1987.32.2.0313

Tylmann, W., Bonk, A., Goslar, T., Wulf, S., Grosjean, M., 2016. Calibrating ^{210}Pb dating results with varve chronology and independent chronostratigraphic markers: Problems and implications. Quat. Geochronol. 32, 1–10.

Tylmann, W., Enters, D., Kinder, M., Moska, P., Ohlendorf, C., Poręba, G., Zolitschka, B., 2013. Multiple dating of varved sediments from Lake Łazduny, northern Poland: Toward an improved chronology for the last 150 years. Quaternary Geochronology 15, 98–107. https://doi.org/10.1016/j.quageo.2012.10.001

Wickham, H., Hester, J., Chang, W., RStudio, R), R.C. team (Some namespace and vignette code extracted from base, 2018. devtools: Tools to Make Developing R Packages Easier.

Wilhelm, B., Arnaud, F., Sabatier, P., Crouzet, C., Brisset, E., Chaumillon, E., Disnar, J.-R., Guiter, F., Malet, E., Reyss, J.-L., Tachikawa, K., Bard, E., Delannoy, J.-J., 2012. 1400 years of extreme precipitation patterns over the Mediterranean French Alps and possible forcing mechanisms. Quat. Res. 78, 1–12.

Wilhelm, B., Sabatier, P., Arnaud, F., 2015. Is a regional flood signal reproducible from lake sediments? Sedimentology 62, 1103–1117. https://doi.org/10.1111/sed.12180

Wilkinson, M.D., Dumontier, M., Aalbersberg, Ij.J., Appleton, G., Axton, M., Baak, A., Blomberg, N., Boiten, J.-W., da Silva Santos, L.B., Bourne, P.E., Bouwman, J., Brookes, A.J., Clark, T., Crosas, M., Dillo, I., Dumon, O., Edmunds, S., Evelo, C.T., Finkers, R., Gonzalez-Beltran, A., Gray, A.J.G., Groth, P., Goble, C., Grethe, J.S., Heringa, J., 't Hoen, P.A.C., Hooft, R., Kuhn, T., Kok, R., Kok, J., Lusher, S.J., Martone, M.E., Mons, A., Packer, A.L., Persson, B., Rocca-Serra, P., Roos, M., van Schaik, R., Sansone, S.-A., Schultes, E., Sengstag, T., Slater, T., Strawn, G., Swertz, M.A., Thompson, M., van der Lei, J., van Mulligen, E., Velterop, J., Waagmeester, A., Wittenburg, P., Wolstencroft, K., Zhao, J., Mons, B., 2016. The FAIR Guiding Principles for scientific data management and stewardship. Scientific Data 3, 160018. https://doi.org/10.1038/sdata.2016.18